Degradation of organic pollutants by a Co_3O_4-graphite composite electrode in an electro-Fenton-like system

LIU Shuan[1,2], GU Yan[1], WANG ShuLian[1], ZHANG Yu[1], FANG YanFen[1], JOHNSON David M[3] & HUANG YingPing[1*]

[1] *Engineering Research Center of Eco-environment in Three Gorges Reservoir Region, Ministry of Education, China Three Gorges University, Yichang 443002, China;*

[2] *Institute of Oceanology, Chinese Academy of Sciences, Qingdao 266071, China;*

[3] *School of Natural Science & Mathematics, Ferrum College, Virginia 24088-9000, USA*

A novel composite electrode was constructed by pressing together Co_3O_4 and graphite and it was used as the cathode in an electro-Fenton-like (EFL) system. The poor electron transport characteristic of Co_3O_4 was overcome by incorporating graphite. *In situ* electro-catalytic generation of hydroxyl radicals ($\cdot OH$) occurred at high current efficiencies from pH 2–10, extending the traditional Fenton reaction pH range. Cyclic voltammetry and AC impedance spectrometry were used to characterize the composite electrode. The ability of the EFL system to degrade organic compounds was investigated using sulforhodamine B (SRB) and 2,4-dichlorophenol (2,4-DCP) as probes. Decoloration of SRB (1.0×10^{-5} mol/L) was complete (100%) in 150 min and SRB was effectively degraded from pH 2–10. The decomposition of SRB was studied using Fourier transform infrared spectroscopy (FT-IR) and total organic carbon (TOC) analysis and results indicated that the final degradation products were carbon dioxide, carboxylic acids and amines. The EFL system also decomposed 2,4-DCP and the degradation was 98.6% in 240 min. Electro-catalytic degradation of SRB occurs by a $\cdot OH$ mechanism. After 5 times reused, the degradation rate of SRB did not significantly slow down. The electrode shows excellent potential for use in advanced oxidation processes (AOPs) used to treat persistent organic pollutants (POPs) in wastewater.

Co_3O_4-graphite electrode, electro-Fenton-like system, electro-generation of hydroxyl radicals, electro-catalytic degradation of POPs

Persistent organic pollutants (POPs) resist conventional chemical and biological treatments and accumulate in the aquatic environment after discharge. They tend to be lipid soluble and undergo food chain amplification and, if toxic, threaten human health. Advanced oxidation processes (AOPs) are among the best advanced treatment technologies because of their ability to mineralize organic pollutants [1,2].
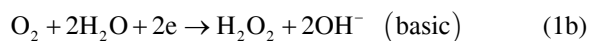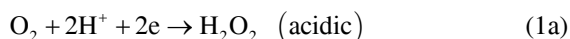
There is widespread interest in producing H_2O_2 *in situ* to lower cost and risk of transportation and increase degrada-

tion efficiency. H_2O_2 generated *in situ* is consumed prior to decomposition to H_2O and O_2, giving higher yields and selectivity for the targeted reactions. Although the classic Fenton reactions (Fe^{2+}/H_2O_2) have been widely used for the treatment of POPs, they have three main drawbacks: the high cost of H_2O_2, the large production of ferric hydroxide sludge and the narrow working pH range [2]. As iron ions precipitates as a hydroxide at higher pH values. Electro-Fenton oxidation method as an indirect electrochemical advanced oxidation process was developed and widely applied for oxidation of POPs. In the EFL process, $\cdot OH$ is formed from the Fenton's reagent which is generated

*Corresponding author (email: huangyp@ctgu.edu.cn)

electrochemically at the cathode. It is strong enough to non-selectively oxide most organic as well as some inorganic compounds [3,4].

In recent years, cobalt oxide (Co_3O_4) has aroused interest because of its unique physical and chemical properties and has been widely used for photocatalysis [5], capacitors [6,7] and fuel cells [8]. Research has shown that the 3d orbitals of Co metal ions display a significant catalytic effect in a Fenton-like system [9,10]. However, the use of cobalt as a cathode material for catalytic reduction of dissolved O_2 to H_2O_2 has been reported rarely, perhaps because of its poor electron transport properties and low current efficiency. In this paper, a new Co_3O_4-graphite electrode was constructed by pressing together electrochemical grade nano-Co_3O_4 and high purity graphite. The electro-catalytic characteristics of the Co_3O_4-graphite electrode were studied using cyclic voltammetry and AC impedance spectroscopy. In the EFL system, the Co_3O_4-graphite electrode acts as the cathode and a Pt net as the anode. Two Co_3O_4-catalyzed cathodic reductions are of interest.

$$O_2 + 2H^+ + 2e \rightarrow H_2O_2 \quad (\text{acidic}) \tag{1a}$$

$$O_2 + 2H_2O + 2e \rightarrow H_2O_2 + 2OH^- \quad (\text{basic}) \tag{1b}$$

$$H_2O_2 + 2e \rightarrow 2 \cdot OH \tag{2}$$

The electro-catalytic degradation of POPs was investigated using sulforhodamine B (SRB) and 2,4-dichlorophenol (2,4-DCP) as probes. Degradation extent of SRB and 2,4-DCP was monitored. The decomposition of SRB was further investigated using Fourier transform infrared spectroscopy (FT-IR) and total organic carbon (TOC) analysis.

1   Experimental

1.1   Materials and reagents

Horseradish peroxidase (POD) was purchased from Hubei Biologic Engineering Co., China, and *N,N*-diethyl-*p*-phenylenediamine (DPD) reagent was provided by Merck Co., Germany. Stock aqueous solutions of sulforhodamine B (SRB) (1.0×10^{-5} mol/L) and 2,4-dichlorophenol (2,4-DCP) (1.0×10^{-3} mol/L) were prepared. All reagents were analytical reagent grade. Double distilled water was used throughout the investigation. The pH of the solution was adjusted with either dilute H_2SO_4 or NaOH.

1.2   Preparation of the Co_3O_4-graphite composite cathode

The Co_3O_4-graphite composite cathode was prepared by loading Co_3O_4 on activate high purified graphite. Co_3O_4 was first prepared by the hydrothermal method according to a procedure reported previously [11]. Nano-Co_3O_4 and graphite were mixed in an ethanol/PTFE emulsion (60% by volume), sonicated for 5 min to disperse the mixture evenly,

and then dried at 50°C to form a dough-like paste. Two pieces of the paste were fixed on a stainless steel mesh current collector and pressed at 30 MPa for 2 min. The electrode was refluxed in acetone for 24 h to remove the ethanol and surface PTFE. The dimensions of the composite electrode were 1.0 $cm^2 \times 5.0$ mm. In addition, X-ray diffraction patterns (XRD) and transmission electron microscopy (TEM) images were used to detect the chemical properties and morphology of the electrode materials. An X-ray diffractometer with Cu Kα radiation ($\lambda = 0.154$ nm) and 10°–80° scanning range was used to obtain XRD patterns. TEM was used to investigate the microstructure of the graphite. The purified graphite was first ultrasonically dispersed to suspend in anhydrous alcohol, then several drops of the suspension were dipped on a 20 nm thick, 3 mm diameter carbon film supported on a copper grid. After they were dried in the air, the samples were observed by Philips EM-420 transmission electron microscope whose operation potential was 80 kV.

1.3   Degradation of SRB and 2,4-DCP

Degradation of SRB and 2,4-DCP in the EFL system were carried out in a divided Pyrex vessel (50 mL) with a two-electrode system. The Co_3O_4-graphite electrode was the cathode and the anode was a 1.0 cm^2 Pt net (99.99% purity, Tianjin Aida Technology Co., Ltd, China). A 10 g/L aqueous solution of Na_2SO_4 was used as the supporting electrolyte. The initial pH of the test solution was 7.0 but was adjusted to study the effect of pH on SRB degradation. The reaction mixture was magnetically stirred at room temperature. Before degradation experiments, the system was stirred for 40 min to establish adsorption/desorption equilibrium between the solution and electrodes in the cathodic cell. A potential of 6 V was applied and 1 mL of sample was removed at set time intervals and analyzed using UV-Vis spectrophotometer (Perkin Elmer, USA) to monitor the degradation of SRB (565 nm). The concentration of 2,4-DCP was measured using the 4-aminoantipyrine colorimetric method [12].

1.4   Analytical methods

The Co_3O_4-graphite electrode was tested using cyclic voltammetry in a three-electrode system. The composite electrode was the working electrode with a Pt counter electrode and saturated calomel as the reference. The electrolyte was 10 g/L Na_2SO_4 and the scanning rate was 50 mV/s. If not stated otherwise, all potentials were reported against SCE (245 mV vs. NHE) in this study. All the experiments were carried out at room temperature (20°C).

AC impedance studies used the same electrode configuration and electrolyte as for cyclic voltammetry. The redox probe was 0.01 mol/L of $K_4Fe(CN)_6$ and $K_3Fe(CN)_6$, the frequency range was 10^5 to 10^{-2} Hz, and the vibration

amplitude was 5 mV.

Mineralization of SRB was measured using Multi N/C 2100 TOC analysis (Jena, Germany) and non-mineralized degradation products were identified using IR-560 spectrophotometry (Nicolet, USA).

The concentration variations of H_2O_2 during the degradation were determined by the DPD method [13]. The fluorescence method [14] was used for the direct detection of ·OH produced to measure indirectly the concentration of ·OH.

2 Results and discussion

2.1 XRD diffraction pattern and TEM image of the electrode materials

The XRD diffraction pattern of the Co_3O_4-graphite composite is shown in Figure 1. The assignment was carried out by using the JCPDS database. The sharp diffraction peak at $2\theta = 26.5°$ was corresponding to high purified graphite (JCPDS No.26-1080). All the remaining diffraction peaks were readily indexed to cubic phase Co_3O_4 (JCPDS No. 42-1467). No obvious peaks of impurities were seen in this pattern, suggesting the high degree of crystallinity of self-made Co_3O_4. Figure 2 shows the TEM image of the high purified graphite. Obviously, the layered structure of graphite had good electron transport properties during the electrocatalytic process.

2.2 Cyclic voltammograms obtained from the Co_3O_4-graphite electrode

Voltammograms of the Co_3O_4-graphite electrode under different pHs are displayed in Figure 3. The cyclic voltammogram is not a regular rectangle, indicating that the capacitance of the Co_3O_4-graphite electrode is a pseudo-capacitance rather than a double layer capacitance. The electrode showed good electro-catalytic properties in the working voltage range. There were the two pairs of redox peaks
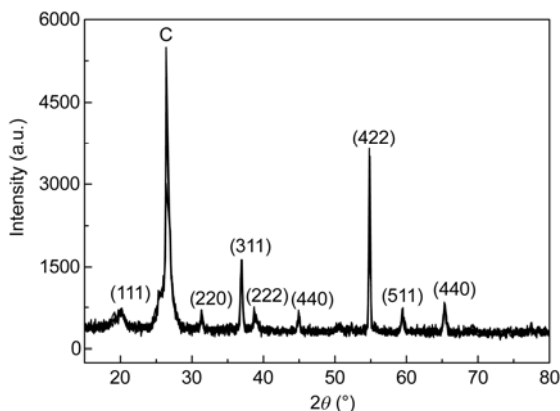

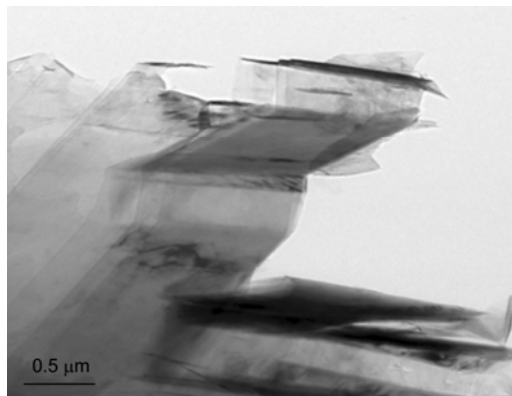**Figure 1**   XRD spectra of the electrode materials.

Figure 2   TEM image of the purified graphite.
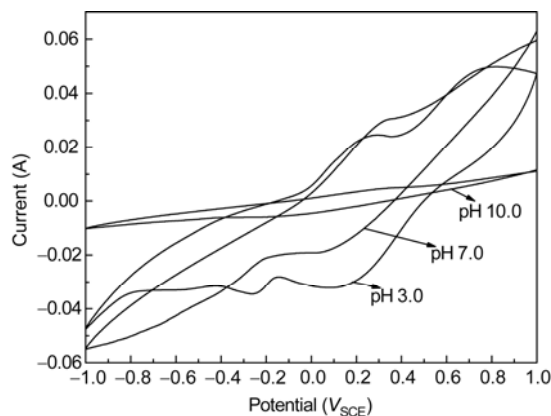

Figure 3   Response of the Co_3O_4-graphite electrode at different pHs.

when the EFL system medium was acidic (pH 3.0). The current peak at 0.18 V vs. SCE is produced by cathodic reduction of O_2 to H_2O_2 (Reaction (1a)) and the current peak at −0.25V vs. SCE is produced by the cathodic reduction of H^+ to H_2. When pH value was adjusted to 7.0 with NaOH, the current peak of H^+/H_2 disappeared because a lower H^+ concentration is accompanied by a corresponding decrease in the reduction of H^+. Increasing the pH to basic conditions (pH 10.0) prevents the reduction of H^+ and decreases the reduction potential of O_2 to 0.12 V vs. SCE (Reaction (1b)), indicating that basic conditions promote the reduction of O_2. Therefore, this EFL system could degrade POPs in a wide pH range.

2.3 AC impedance spectra of the Co_3O_4-graphite electrode

Using $K_4Fe(CN)_6$ and $K_3Fe(CN)_6$ as the redox probe and Na_2SO_4 (10 g/L) as the electrolyte, the AC impedance spectra of three electrodes (graphite, Co_3O_4, and Co_3O_4-graphite) were obtained and are displayed in Figure 4.

The high frequency arc corresponds to the ohmic resistance and contact resistance of a porous electrode, and is a sign of dynamic control. The curves correspond to Faraday
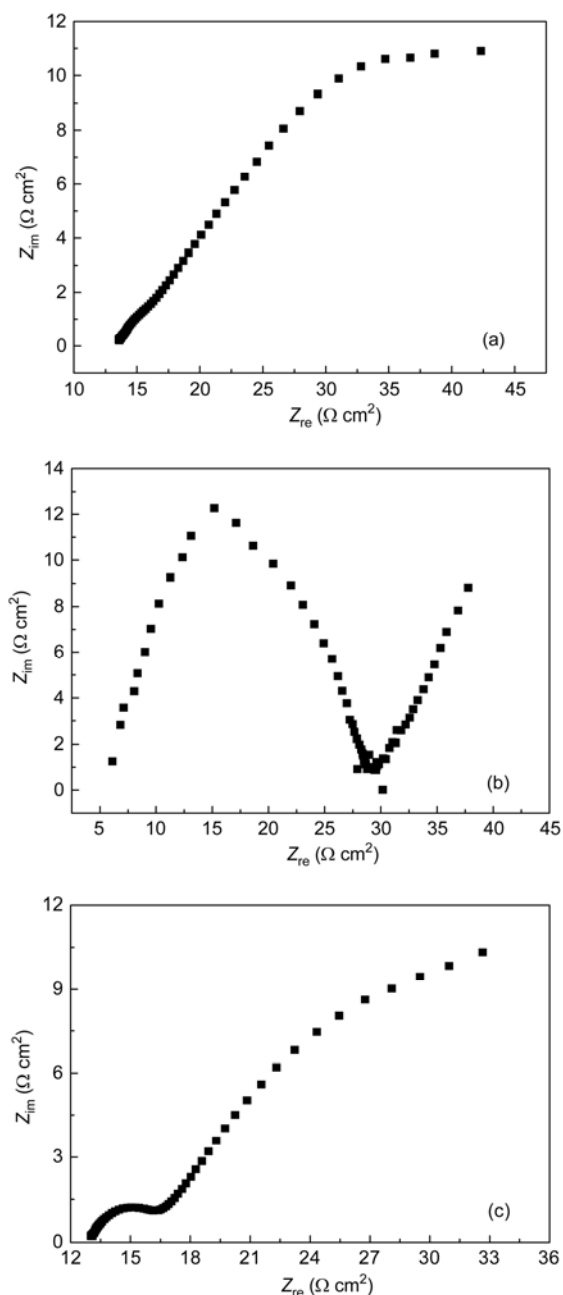
by diffusion. Again under the same conditions, the AC impedance curve for the Co_3O_4-graphite composite electrode displayed a small peak in the high frequency area with a nearly linear response at low frequencies, indicating dynamic control at high frequencies and diffusion control at low frequencies. Comparing the AC impedance spectra of three different electrode, Co_3O_4 hinders electron exchange between $K_4Fe(CN)_6/K_3Fe(CN)_6$ and the electrode but the hindrance is removed in the Co_3O_4-graphite electrode by the good electron transport properties of graphite. In short, the Co_3O_4-graphite electrode displays good electrochemical response.

2.4   Degradation of SRB in EFL system

The absorption spectrum changes accompanying degradation of SRB in the electro-Fenton system are displayed in Figure 5. The spectrum of SRB is characterized by a maximum absorption peak at 565 nm in the visible region and two smaller peaks locate at 260 nm and 285 nm in the ultraviolet region. The latter two peaks are ascribed to the $\pi-\pi^*$ transition related to the conjugated double bonds (C=C) in the dye molecule. The band in visible region is attributed to the ethyl containing azo linkage of the dye molecules. With increased reaction time, the absorption peak at 565 nm decreases, indicating degradation of SRB by cleavage of the azo linkage. This finding is significant in the search for new techniques to remove azo dyes with N–N bonds. The intensity of absorption at 260 and 285 nm also gradually decrease and then disappear, indicating that the macromolecular structure of SRB has been destroyed.

2.5   Effect of electrode composition on the degradation of SRB

To study the effect of electrode composition (mass ratio of Co_3O_4 to graphite) on the degradation of SRB, various composite ratios were tested in the EFL system. The results are showed in Figure 6 and indicate that a Co_3O_4 to graphite
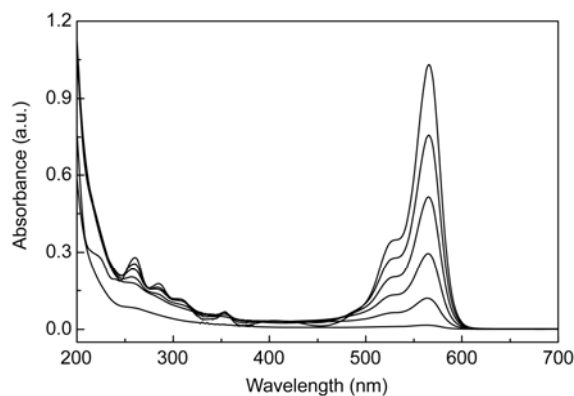
Figure 4   AC impedance curves of different electrodes. (a) Graphite electrode; (b) Co_3O_4 electrode; (c) Co_3O_4-graphite electrode.

impedance and the double layer capacitance of the three-phase reaction zone and indicate diffusion control [15,16]. The AC impedance curve of the graphite electrode was a straight line throughout the frequency range, indicating that $K_4Fe(CN)_6$ and $K_3Fe(CN)_6$ exchange electrons quickly. The graphite electrode has good electron transport properties and the electrode reaction rate is controlled by diffusion. Under the same conditions, the AC impedance curve of the Co_3O_4 electrode displayed a large peak in the high frequency range, indicating that the Co_3O_4 electrode has a large resistance and that the electrode reaction process is controlled

Figure 5   Temporal absorption spectral changes of SRB. *U*=6.0 V, pH= 7.0, [Na_2SO_4]=10 g/L, [SRB]=1.0×10^{-5} mol/L.
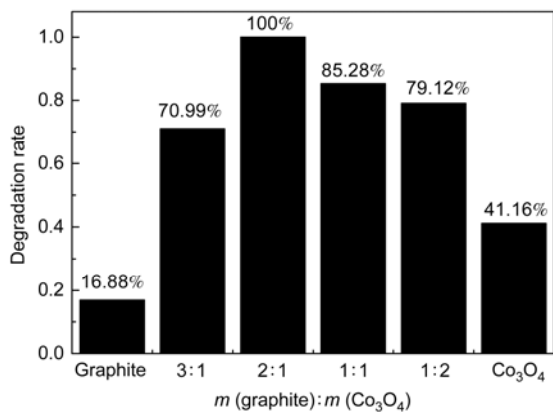
Figure 6 Effect of electrode composition on the degradation of SRB. U=6.0 V, pH=7.0, [Na$_2$SO$_4$]=10.0 g/L, [SRB]=1.0×10^{-5} mol/L.

mass ratio of 2:1 is most effective.

2.6 Effect of pH on the degradation of SRB

The pH plays an important role in Fenton systems [17,18]. The traditional Fenton reaction has high catalytic activity only under acidic conditions (pH 2–3). However, the optimum condition for the electrochemical generation of H$_2$O$_2$ in the EFL system is in the basic pH range. The influence of initial pH on degradation efficiency of SRB in the electro-Fenton system was investigated. Assuming that the degradation of SRB follows pseudo-first-order kinetics, the dynamic curve are displayed in Figure 7 and indicate that SRB degradation efficiency was not pH dependent and that this new electro-Fenton system performed effectively from pH 2–10, the kinetic constants for the electro-Fenton system under different pH values were calculated and are summarized in Table 1. The kinetic constant at pH 2–3 was 2.972× 10^{-2} min^{-1} and the degradation of SRB was 100%. When the pH was adjusted to neutral and basic conditions, the kinetic constant decreased to 1.41×10^{-2} min^{-1}, but the degradation
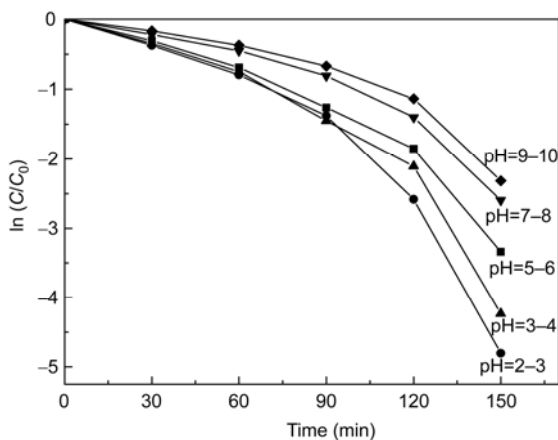

Figure 7 Effect of pH on the degradation of SRB. U=6.0 V, pH=7.0, [Na$_2$SO$_4$]=10.0 g/L, [SRB]=1.0×10^{-5} mol/L.

Table 1 Pseudo-first-order rate constants, regression coefficients, and extent of SRB degradation (after 150 min) in the EFL system at various pH values

pH	Kinetic constant (min^{-1})	Coefficient (R)	Degradation of SRB (%)
2–3	0.02972	0.9341	100
3–4	0.02586	0.9374	98.55
5–6	0.02086	0.9564	96.46
7–8	0.01607	0.9397	92.55
9–10	0.01408	0.9258	90.14

still exceeded 90%. The reduction potential of O$_2$ decreases and current efficiency improved under neutral and basic conditions. The EFL system with Co$_3$O$_4$-graphite cathode performs in basic conditions without loss of efficiency.

2.7 Concentration of oxidizing species during the degradation of SRB

The effectiveness of the Fenton reaction depends on catalytic generation of H$_2$O$_2$, which then yields the highly reactive ·OH that oxidizes organic material non-selectively [19]. In the EFL system, the electro-generated levels of H$_2$O$_2$ and ·OH determine the rate and efficiency of SRB degradation. Figure 8 displays the concentration changes of H$_2$O$_2$ and relative content of ·OH as the degradation reaction proceeds [20,21]. There was no H$_2$O$_2$ or ·OH generated when no voltage was applied to the electrode (Figure 8(b)). When 6 V voltage was applied, the concentration of H$_2$O$_2$, generated by cathodic reduction increased with time (Figure 8(a)). Approximately 90 min later, the H$_2$O$_2$ concentration reached a steady state and then decreased. This indicates that H$_2$O$_2$ production increased in the beginning and then consumed in the degradation of SRB. Comparing Figure 8(a) and (b) it can be seen that the H$_2$O$_2$ electro-generated in the EFL system was quickly converted to ·OH. The degradation of SRB in the EFL system are characteristic of the Fenton reaction and indicate that the degradation process involves ·OH.

2.8 Mineralization of SRB

To measure the extent of SRB mineralization in the EFL system, the change of solution TOC was tracked during degradation and results are displayed in Figure 9. The TOC did not change when no voltage was applied to the electrode but when 6 V was applied the mineralization rate of SRB was 55.5% in 5 h. These results suggested that the EFL system not only discolored the SRB but oxidized over half the dye to CO$_2$ (mineralization).

2.9 Identification of non-mineralized SRB degradation products
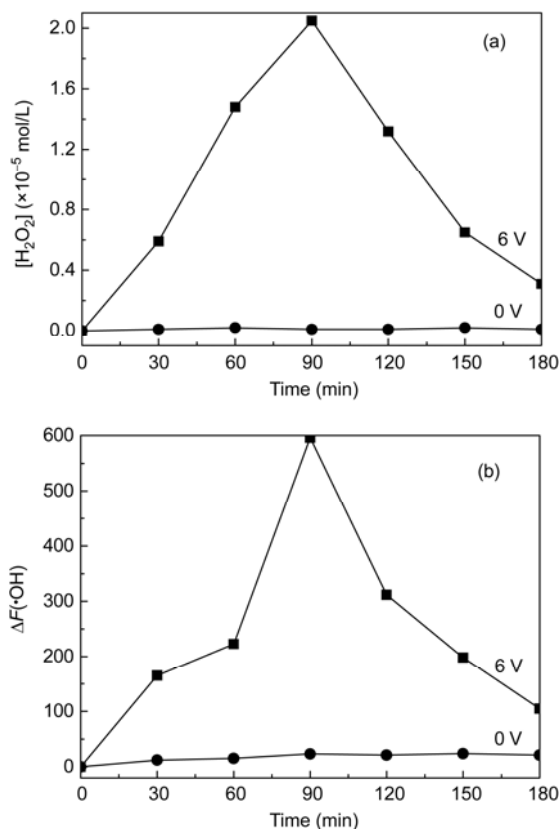
FTIR was used to identify non-mineralized products as the

Figure 8   Concentration of H_2O_2 (a) and relative content of ·OH (b). U=6.0 V, pH=7.0, [Na_2SO_4]=10.0 g/L, [SRB]=1.0×10^{-5} mol/L.
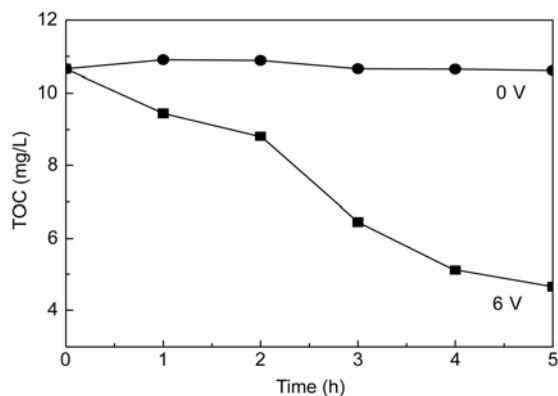
Figure 9   TOC removal of SRB. U=6.0 V, pH=7.0, [Na_2SO_4]=10.0 g/L, [SRB]=2.0×10^{-5} mol/L.

degradation proceeded and the results are displayed in Figure 10. Initially, bands at 1640–1650 cm^{-1} and 1600, 1480–1500, 1450 cm^{-1} indicate aromatic-N ring vibration and skeleton vibration of the SRB molecule, respectively. The absorption peak at 1090–1100 cm^{-1} indicates the existence of C–O–C stretching and the band at 1120–1140 cm^{-1} and 620–670 cm^{-1} indicate the presence of the –SO$_3$ group. As the electro-catalytic reaction preceded, the bands of 1650, 1600 and 1100 cm^{-1} disappeared after 3 h indicting the cleavage of nitrogen and C–O–C from the aromatic ring. At
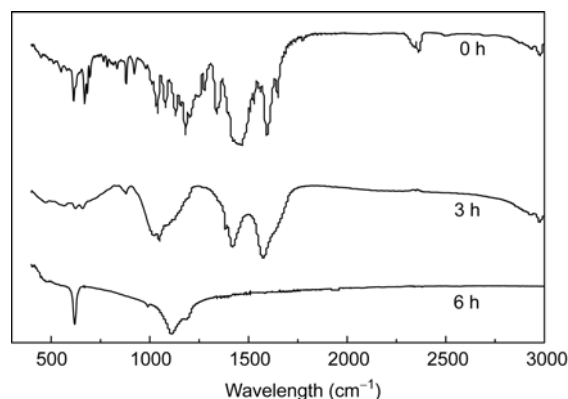

Figure 10   IR spectra of SRB during degradation. U=6.0 V, pH=7.0, [Na_2SO_4]=10.0 g/L, [SRB]=1.0×10^{-5} mol/L.

the same time, the appearance of new absorbance bands at 850 and 1400 cm^{-1} correspond to the –CH$_2$– in ethylenediamine. Further, the C=O absorption peak at 1600–1700 cm^{-1} grew larger. Six hours later, the bands at 850, 1400 and 1600–1700 cm^{-1} were gone. The IR spectra show that SRB not mineralized is decomposed to carboxylic acids and small amines.

2.10   Degradation of 2,4-DCP

2,4-DCP is a toxic persistent non-biodegradable organic pollutant (POP) and was used to evaluate the electro-catalytic effectiveness of the EFL system toward such substances. Levels of 2,4-DCP were monitored during degradation by measuring solution absorption at 265 nm. The decomposition curves of 2,4-DCP in a neutral EFL system with Co$_3$O$_4$-graphite cathode are displayed in Figure 11. The decomposition of 2,4-DCP was negligible when no voltage was supplied to the electrodes. When 6 V voltage was supplied, 2,4-DCP decomposition was 98.8% after 210 min, indicating that the EFL system could effectively degrade 2,4-DCP.
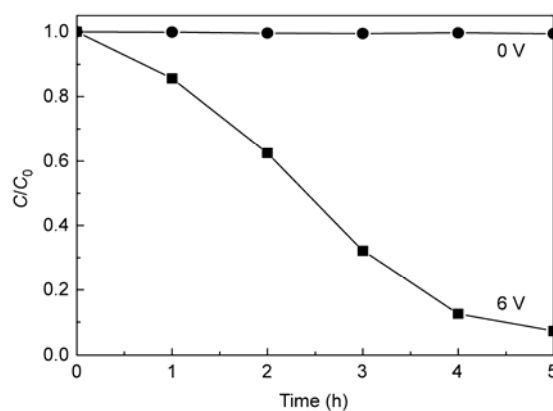

Figure 11   Degradation of 2,4-DCP by the EFL system. U=6.0 V, pH=7.0, [Na_2SO_4]=10.0 g/L, [2,4-DCP]=1.0×10^{-3} mol/L.
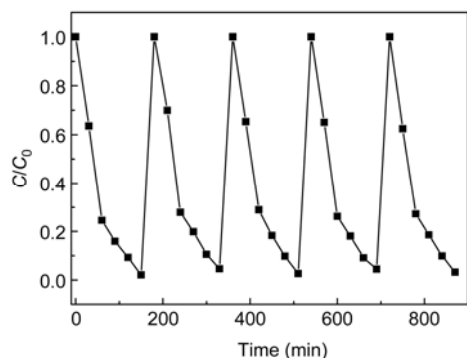
Figure 12 The stability of Co_3O_4-graphite electrode. U=6.0 V, pH=7.0, [Na_2SO_4]=10.0 g/L, [SRB]=2.0×10^{-5} mol/L.

2.11 Stability of Co_3O_4-graphite electrode

The stability of electrode is the key to its practical application, in order to study the stability of Co_3O_4-graphite electrode, the degradation of SRB by the same Co_3O_4-graphite electrode under the same conditions is also evaluated (Figure 12). After 5 times reused, the degradation rate of SRB did not significantly slow down, indicating that the electrode can be reused and have good stability.

3 Conclusions

The EFL system, with a Co_3O_4-graphite composite cathode, degraded the organic dye SRB and persistent organic compound 2,4-DCP effectively. The ability of the EFL system to efficiently generate H_2O_2 and ·OH in situ and to cleave the N–N bond in SRB are both significant. The Co_3O_4-graphite composite electrode displays good electrochemical characteristics and produces H_2O_2 and ·OH from pH 2–10. The system extends the traditional Fenton reaction pH range and the composite electrode displays high current efficiency. These characteristics give the Co_3O_4-graphite composite electrode excellent potential in advanced oxidation processes used to treat water and wastewater containing persistent organic pollutants.

1　Khataee A R, Safarpour M, Zarei M, et al. Electrochemical generation of H_2O_2 using immobilized carbon nanotubes on graphite electrode fed with air: Investigation of operational parameters. J Electroanal Chem, 2011, 659: 63–68

2　Wang S L, Fang Y F, Yang Y, et al. Catalysis of organic pollutant photodegradation by metal phthalocyanines immobilized on TiO_2@-SiO_2. Chin Sci Bull, 2011, 56: 969–976

3　Khataee A R, Zarei M, Asl S K. Photocatalytic treatment of a dye solution using immobilized TiO_2 nanoparticles combined with photo-electro-Fenton process: Optimization of operational parameters. J Electroanal Chem, 2010, 648: 143–150

4　Iranifam M, Zarei M, Khataee A R, et al. Basic Yellow 28 solution using supported ZnO nanoparticles coupled with photoelectro-Fenton process. J Electroanal Chem, 2011, 659: 107–112

5　Huang Y H, Huang Y F, Huang C I, et al. Efficient decolorization of azo dye Reactive Black B involving aromatic fragment degradation in buffered Co^{2+}/PMS oxidative processes with a ppb level dosage of Co^{2+}-catalyst. J Hazard Mater, 2009, 170: 1110–1118

6　Ahn H J, Seong T Y. Effect of Pt nanostructures on the electrochemical properties of Co_3O_4 electrodes for micro-electrochemical capacitors. J Alloy Compd, 2009, 478: 8–11

7　Wang L, Liu X H, Wang X, et al. Preparation and electrochemical properties of mesoporous Co_3O_4 crater-like microspheres as supercapacitor electrode materials. Curr Appl Phys, 2010, 10: 1422–1426

8　Kobayashi M, Hidai S, Niwa H, et al. Co oxidation accompanied by degradation of Pt-Co alloy cathode catalysts in polymer electrolyte fuel cells. Phys Chem Chem Phys, 2009, 11: 8226–8230

9　Bandala E R, Pelaez M A, Salgado M J, et al. Degradation of sodium dodecyl sulfate in water using solar driven Fenton-like advanced oxidation processes. J Hazard Mater, 2008, 151: 578–584

10　Ling S K, Wang S B, Peng Y L. Oxidative degradation of dyes in water using Co^{2+}/H_2O_2 and Co^{2+}/peroxymonosulfate. J Hazard Mater, 2010, 178: 385–389

11　Zhang W M, Sun S X, Yu H Y, et al. Synthesis of Co_3O_4 nanopowder with different morphologies by hydrothermal treatment followed by decomposition (in Chinese). Chem J Chinese U, 2003, 12: 2451–2154

12　Munaf E, Zein R, Kurniadi R, et al. The use of rice husk for removal of phenol from wastewater as studied using 4-aminoantipyrine spectrophotometric method. Environ Sci Technol, 1997, 18: 355–358

13　Bader H, Sturzenegger V, Hoigne J. Photometric method for the determination of low concentrations of hydrogen peroxide by the peroxidase catalyzed oxidation of *N,N*-diethyl-*p*-phenylenediamine (DPD). Water Res, 1988, 22: 1109–1115

14　Ishibashi K, Fujishima A, Watanabe T, et al. Detection of active oxidative species in TiO_2 photocatalysis using the fluorescence technique. Electrochem Commun, 2000, 2: 207–210

15　Huang H, Zhang W K, Zhao F M, et al. Electrocatalytic performances of carbon nanotube air electrode for oxygen reduction (in Chinese). Chinese J Appl Chem, 2002, 19: 759–763

16　Liu S, Sun H Y, Sun L J, et al. Effects of pH and Cl$^-$ concentration on corrosion behavior of the galvanized steel in simulated rust layer solution. Corros Sci, 2012, 65: 520–527

17　Cheng Z Y, Li Y Z, Chang W B. Kinetic deoxyribose degradation assay and Its application in assessing the antioxidant activities of phenolic compounds in a Fenton-type reaction system. Anal Chim Acta, 2003, 478: 129–137

18　Anipsitakis G P, Dionysiou D D. Degradation of organic contaminants in water with sulfate radicals generated by the conjunction of peroxymonosulfate with cobalt. Environ Sci Technol, 2003, 37: 4790–4797

19　Ai Z H, Lu L R, Li J P, et al. Fe@Fe_2O_3 core-shell nanowires as iron reagent. 1. Efficient degradation of rhodamine B by a novel sono-Fenton process. J Phys Chem C, 2007, 111: 4087–4093

20　Ai Z H, Lu L R, Li J P, et al. Fe@Fe_2O_3 core-shell nanowires as iron reagent. 2. An efficient and reusable sono-Fenton System working at neutral pH. J Phys Chem C, 2007, 111: 7430–7436

21　Ai Z H, Mei T, Liu J, et al. Fe@Fe_2O_3 core-shell nanowires as iron reagent. 3. Their combination with CNTs as an effective oxygen-fed gas diffusion electrode in a neutral EFL system. J Phys Chem C, 2007, 111: 14799–14803